Journal of Computer-Aided Molecular Design **18:** 615–634, 2004.
DOI 10.1007/s10822-004-5171-y

TOMOCOMD-CARDD, a novel approach for computer-aided 'rational' drug design: I. Theoretical and experimental assessment of a promising method for computational screening and *in silico* design of new anthelmintic compounds

Yovani Marrero-Ponce[a,b,*], Juan A. Castillo-Garit[b,c], Ervelio Olazabal[d], Hector S. Serrano[d], Alcidez Morales[d], Nilo Castañedo[b,d], Froylán Ibarra-Velarde[e], Alma Huesca-Guillen[e], Elisa Jorge[a], Arletys del Valle[a], Francisco Torrens[f] & Eduardo A. Castro[g]

[a]*Department of Pharmacy, Faculty of Chemical-Pharmacy, Central University of Las Villas, Santa Clara 54830, Villa Clara, Cuba;* [b]*Department of Drug Design, Chemical Bioactive Center, Central University of Las Villas, Santa Clara 54830, Villa Clara, Cuba;* [c]*Applied Chemistry Research Center, Central University of Las Villas, Santa Clara 54830, Villa Clara, Cuba;* [d]*Department of Parasitology, Chemical Bioactive Center, Central University of Las Villas, Santa Clara 54830, Villa Clara, Cuba;* [e]*Department of Parasitology, Faculty of Veterinarian Medicinal and Zootecnic. UNAM, Mexico, D.F. 04510, Mexico;* [f]*Institut Universitari de Ciència Molecular, Universitat de València, Dr. Moliner 50, E-46100 Burjassot (València), Spain;* [g]*INIFTA, División Química Teórica, Suc.4, C.C.16, La Plata 1900, Buenos Aires, Argentina*

Received 4 August 2004; accepted in revised form 21 October 2004

Key words: anthelmintic activity, QSAR, *TOMOCOMD-CARDD* software, total and local quadratic indices, virtual screening

Summary

In this work, the *TOMOCOMD-CARDD* approach has been applied to estimate the anthelmintic activity. Total and local (both atom and atom-type) quadratic indices and linear discriminant analysis were used to obtain a quantitative model that discriminates between anthelmintic and non-anthelmintic drug-like compounds. The obtained model correctly classified 90.37% of compounds in the training set. External validation processes to assess the robustness and predictive power of the obtained model were carried out. The QSAR model correctly classified 88.18% of compounds in this external prediction set. A second model was performed to outline some conclusions about the possible modes of action of anthelmintic drugs. This model permits the correct classification of 94.52% of compounds in the training set, and 80.00% of good global classification in the external prediction set. After that, the developed model was used in virtual *in silico* screening and several compounds from the Merck Index, Negwer's handbook and Goodman and Gilman were identified by models as anthelmintic. Finally, the experimental assay of one organic chemical (**G-1**) by an *in vivo* test coincides fairly well (100%) with model predictions. These results suggest that the proposed method will be a good tool for studying the biological properties of drug candidates during the early state of the drug-development process.

*To whom correspondence should be addressed. Fax: +53-42-281130, 281455; E-mail: yovanimp@qf.uclv.edu.cu, ymarrero77@cyahoo.es

Introduction

Helminth infections are a medical and public health problem of high magnitude, in both humans and domestic animals [1]. Anthelmintic drugs are used to control, prevent and treat nematode, cestode and trematode parasite infestations in humans and animals [2]. Regrettably with the increased use of these compounds, anthelmintic resistance (see Table 1) has appeared and increased in frequency [3]. If resistance to a particular anthelmintic has occurred, it is likely that another anthelmintic with the same mode of action will also be ineffective, although other anthelmintics with another mode of action may still be effective [4]. In addition, continued economic losses in animal production and human diseases due to parasites are still of concern to industrial chemists looking for new anthelmintic agents [2]. The great cost associated with the development of new compounds and the small economic size of the market for anthelmintics makes this development slow. For instance, no fasciolicide has been marketed since the 1980s [5].

At present, it is not possible to carry out a rigorous classification of the anthelmintic drugs according to their mechanisms of action. However, there are two major modes of action of these drugs: (a) the first group acts on the ion channels of parasite membranes and usually has more rapid therapeutic effect, and (b) the second group acts more slowly within a range of biochemical target sites found in parasites [2]. Table 2 depicts the different modes of action of anthelmintic drugs.

An alternative to the 'real' world of synthesis and screening of compounds in the laboratory is an *in silico* 'virtual' world of data, analysis, hypothesis and design that reside inside a computer. By this means, ''the expensive commitment to actual synthesis and bioassay is made only after exploring the initial concepts with computational models and screens'' [27, 28]. This *in silico* procedure will be used here in order to find predictive models that permit the 'rational' selection/identification or design of new anthelmintics with the required properties.

Recently, one of the present authors has introduced the novel computer-aided molecular design scheme *TOMOCOMD-CARDD* (acronym of *TO*pological *MO*lecular *COM*puter *D*esign-*C*omputer *A*ided '*R*ational' *D*rug *D*esign) [29]. It calculates several new families of topological molecular descriptors. One of these families has been defined as molecular quadratic indices by analogy with the mathematical quadratic forms [30]. This point of view was successfully applied to the prediction of physical properties and Caco-2

Table 1. Resistances to anthelmintics.

Host	Parasite	Drug
Humans	Schistosomes [6, 7]	Oxamniquine
		Praziquantel
	Hookworms [8, 9]	Tetrahydropyrimidines
Sheep and goats	Trichostrongylids [10, 11]	Benzimidazoles
		Levamisole
		Tetrahydropyrimidines
		Macrocyclic lactones
	Fasciola [10, 12, 13]	Benzimidazoles
		Triclabendazol
		Closantel
Extensive grazing pigs	Trichostrongylids [10, 11]	Benzimidazoles
		Macrocyclic lactones
	Oesophagostomum [10, 11]	Benzimidazoles
		Macrocyclic lactones
		Tetrahydropyrimidines
Horses	Small strongyles [10, 11]	Benzimidazoles
		Tetrahydropyrimidines
		Piperazine

Table 2. Anthelmintics target sites.

Target site (and parasite group)	Generic drug name
Ion-channel target sites	
Nicotinic acetylcholine receptor (in nematodes) [14–16]	Levamisole, Butamisole, Pyrantel, Morantel, Bephenium, Thenium, Methyridine
GABA receptors (in large intestinal nematodes) [17]	Piperazine
$GluCl^-$ receptor (in nematodes and insect parasites) [18, 19]	Ivermectin, Abamectin, Doramectin, Moxidectin
Membrane calcium permeability (in cestodes and trematodes) [20]	Praziquantel
Target sites other than ion-channels	
β-Tubulina (in nematodes)	Thiabendazole, Cambendazole, Oxibendazole, Albendazole, Albendazole sulfoxide
β-Tubulina (in nematodes, cestodes and trematodes) [21]	Fenbendazole, Oxfendazole, Mebendazole, Flubendazole, Febantel, Netobimin, Thiofanate, Triclabendazole
Proton ionophores (concentrated and effective against blood feeders: Flukes, *Haemonchus contortus*, *Oestrus ovis*) [22]	Closantel, Hexaclorophene, Oxiclozanida, Rafoxanide, Dibromosalan, Niclosamide, Brotianida, Niclofolan, Nitroxynil
Malate metabolism (in immature fasciola) [23, 24]	Diamfenetide
Phosphoglycerate kinase and mutase [25]	Clorsulon
Arachidonic acid metabolism and innate immunity of host (effective against filaria) [26]	Diethylcarbamazina

permeability of organic compounds and drugs, respectively [30–32]. The method is flexible and enables the study of small molecules as well as macromolecules such as nucleic acids [33].

The main aims of this paper are the following: (1) to develop a quantitative model that discriminates anthelmintic compounds from the inactive ones using the *TOMOCOMD-CARDD* approach and linear discriminant analysis (LDA), and (2) to perform another LDA model in order to classify organic chemicals according to their anthelmintic mode of action. After that, a simulated experimental virtual (computational) screening for search of anthelmintic drugs is conducted by using the models developed here. Finally, the identification and biological evaluation of a novel 2-furylethylene derivative compound (**G-1**) with anthelmintic activity are presented.

Theoretical approach

The general principles of the quadratic indices of the 'molecular pseudograph's atom adjacency matrix' for small-to-medium sized organic compounds have been explained in some detail elsewhere [30–32]. However, an overview of this approach will be given. The molecular vector (X) is constructed in order to calculate the molecular quadratic indices for a molecule where the components of this vector are numeric values, which represent a certain atomic property. Such properties can be the electronegativity, atomic radius, and so on.

If a molecule consists of n atoms (*vector of* $\Re^n$), then the kth total quadratic indices, $\boldsymbol{q}_{\mathbf{k}}(\mathrm{x})$ are calculated as a quadratic form $(q : \Re^n \rightarrow \Re)$ in canonical basis as shown in Equation 1:

$$q_k(x) = \sum_{i=1}^{n} \sum_{j=1}^{n} {}^{k}a_{ij}\, X_i\, X_j \qquad (1)$$

where ${}^{k}a_{ij} = {}^{k}a_{ji}$ (symmetric square matrix), n is the number of atoms of the molecule and $X_1,\ldots,X_{\mathrm{n}}$ are the coordinates of the molecular vector (X) in canonical ('natural') bases of the $\Re^n$. For that reason, those coordinates can be considered as weights (atom-labels) of the vertices of the pseudograph.

The coefficients ${}^{k}a_{\mathrm{ij}}$ are the elements of the kth power of the matrix $\mathbf{M}(\mathrm{G})$ of the molecular pseudograph (G). Here, $\mathbf{M}(\mathrm{G}) = \mathbf{M} = [a_{ij}]$, denotes the

matrix of $\boldsymbol{q_k}(x)$ with respect to the natural basis. In this matrix n is the number of vertices (atoms) of G and the elements a_{ij} are defined as follows [30–32]:

$$\begin{aligned} a_{ij} &= P_{ij} \text{ if } i \neq j \text{ and } \exists\, e_k \in \mathrm{E(G)} \\ &= L_{ii} \text{ if } i = j \\ &= 0 \text{ otherwise} \end{aligned} \tag{2}$$

where E(G) represents the set of edges of G. P_{ij} is the number of edges between vertices v_i and v_j and L_{ii} is the number of loops in v_i.

Given that $a_{ij} = P_{ij}$, the elements a_{ij} of this matrix represent the number of bonds between an atom i and an atom j. The matrix $\mathbf{M^k}$ provides the number of walks of length k that link the vertices v_i and v_j. For this reason, each edge in $\mathbf{M^1}$ represents 2 electrons belonging to the covalent bond between atoms (vertices) v_i and v_j, for example, the inputs of $\mathbf{M^1}$ are equal to 1, 2 or 3 when single, double or triple bonds appear between vertices v_i and v_j, respectively. On the other hand, molecules containing aromatic rings with more than one canonical structure are represented like a pseudograph. This occurs for substituted aromatic compounds such as pyridine, naphthalene, quinoline, and so on, where the presence of pi (π) electrons is accounted for by means of loops in each atom of the aromatic ring. Conversely, aromatic rings having only one canonical structure, such as furan, thiophene and pyrrol are represented like a multigraph.

On the other hand, the defining Equation 1 for $q_k(x)$ may be written as the single matrix equation

$$q_k(x) = [X_1 \cdots X_n] \begin{bmatrix} a_{11} & \cdots & a_{1n} \\ \vdots & & \vdots \\ a_{n1} & \cdots & a_{nn} \end{bmatrix}^k \begin{bmatrix} X_1 \\ \vdots \\ X_n \end{bmatrix} \tag{3}$$

or in the more compact form

$$\boldsymbol{q_k}(x) = [\mathrm{X}]^{\mathrm{t}} \mathbf{M^k} [\mathrm{X}] \tag{4}$$

where [X] is a column vector (an $n \times 1$ matrix) of the coordinates of X in the canonical basis of $\Re^n$, $[\mathrm{X}]^{\mathrm{t}}$ the transpose of [X] (an $1 \times$ n matrix) and $\mathbf{M}^k$ the kth power of the matrix $\mathbf{M}$ of the molecular pseudograph G (matrix in mathematical quadratic form). In Table 3 the calculation of six quadratic indices for acetylsalicylic acid is exemplified.

In addition to a total quadratic index computed for the whole molecule, a local-fragment (atom and atom-type) formalism can be developed. These descriptors are termed local quadratic indices of the 'molecular pseudograph's atom adjacency matrix', $\boldsymbol{q_{kL}}(x)$. The $\boldsymbol{q_{kL}}(x)$ are graph-theoretical invariants for a given fragment F_R (connected subgraph) within a specific pseudograph G. The definition of these descriptors is as follows:

$$\boldsymbol{q}_{kL}(x) = \sum_{i=1}^{m} \sum_{j=1}^{m} {}^k a_{ijL}\, X_i\, X_j \tag{5}$$

where m is the number of atoms in the fragment of interest and ${}^k\boldsymbol{a}_{ijL}$ is the element of the ith row and jth column of the matrix $\mathbf{M}_L^k = \mathbf{M}^k(\mathrm{G}, F_R)$ [$\boldsymbol{q}_{kL}(x) = \boldsymbol{q}_k(x, F_R)$]. This matrix is extracted from the $\mathbf{M^k}$ matrix; it contains the information referring to the vertices of the specific molecular fragment (F_R) and of the molecular environment. The matrix $\mathbf{M}_L^k = [{}^k\boldsymbol{a}_{ijL}]$ with elements ${}^k\boldsymbol{a}_{ijL}$ is defined as follows:

$$\begin{aligned} {}^k a_{ijL} &= {}^k a_{ij} \text{ if both } v_i \text{ and } v_j \text{ are vertices} \\ &\qquad \text{contained within } F_R \\ &= 1/2^k a_{ij} \text{ if } v_i \text{ or } v_j \text{ is contained within } F_R \\ &= 0 \text{ otherwise} \end{aligned} \tag{6}$$

with ${}^k a_{\mathrm{ij}}$ being the elements of the kth power of $\mathbf{M}$. These local analogues can also be expressed in matrix form by the expression

$$\boldsymbol{q}_{kL}(x) = [\mathrm{X}]^{\mathrm{t}} \mathbf{M}_L^k [\mathrm{X}] \tag{7}$$

Note that for every partitioning of a molecule into Z molecular fragments there will be Z local molecular fragment matrices. That is to say, if a molecule is partitioned into Z molecular fragments, the matrix $\mathbf{M^k}$ can be partitioned into Z local matrices $\mathbf{M}_L^k$, $\mathbf{L} = 1, \ldots, \mathrm{Z}$ and the kth power of matrix $\mathbf{M}$ is exactly the sum of the kth power of the local ('molecular fragment') Z matrices

$$\mathbf{M^k} = \sum_{L=1}^{z} M_L^k \tag{8}$$

or in the same way as $\mathbf{M^k} = [{}^k a_{ij}]$, where

$${}^{\boldsymbol{k}}\boldsymbol{a}_{\boldsymbol{ij}} = \sum_{L=1}^{z} {}^k a_{ijL} \tag{9}$$

and the total quadratic index is the sum in the quadratic indices of the Z molecular fragments

$$\boldsymbol{q_k}(x) = \sum_{L=1}^{z} q_{kL}(x) \tag{10}$$

Table 3. Definition and calculation of six (k = 0–5) total quadratic indices of the molecular pseudograph's atom adjacency matrix of the molecule of acetylsalicylic acid.

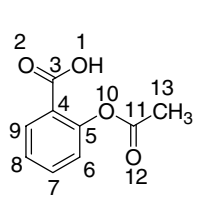

Acetylsalicylic Acid

Molecular structure

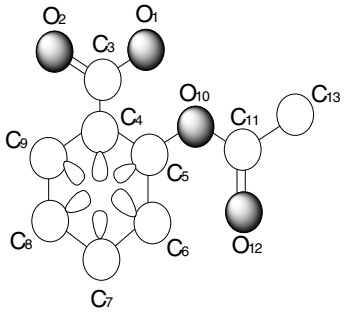

Molecular Pseudograph (G)
(Suppressed Hydrogen Atom)

$$q_0(x) = \sum_{i=1}^{n}\sum_{j=1}^{n} {}^0a_{ij}X_iX_j = [X]^tM^0[X] = 102.4472$$

$$q_1(x) = \sum_{i=1}^{n}\sum_{j=1}^{n} {}^1a_{ij}X_iX_j = [X]^tM^1[X] = 268.8912$$

$$q_2(x) = \sum_{i=1}^{n}\sum_{j=1}^{n} {}^2a_{ij}X_iX_j = [X]^tM^2[X] = 373.5982$$

$$q_3(x) = \sum_{i=1}^{n}\sum_{j=1}^{n} {}^3a_{ij}X_iX_j = [X]^tM^3[X] = 2566.8034$$

$$q_4(x) = \sum_{i=1}^{n}\sum_{j=1}^{n} {}^4a_{ij}X_iX_j = [X]^tM^4[X] = 8381.1414$$

$$q_5(x) = \sum_{i=1}^{n}\sum_{j=1}^{n} {}^5a_{ij}X_iX_j = [X]^tM^5[X] = 25593.612$$

$\mathbf{X} = [O_1\ O_2\ C_3\ C_4\ C_5\ C_6\ C_7\ C_8\ C_9\ O_{10}\ C_{11}\ O_{12}\ C_{13}]$

Molecular Vector: $\mathbf{X} \in \Re$

In the definition of the **X**, as molecular vector, the chemical symbol of the element is used to indicate the corresponding electronegativity value. That is: if we write O it means χ(O), oxygen Mulliken electronegativity or some atomic property, which characterizes each atom in the molecule. So, if we use the canonic bases of R, the coordinates of any vector **X** coincide with the components of that molecular vector

$[X]^t$ = [3.17 3.17 2.63 2.63 2.63 2.63 2.63 2.63 2.63 3.17 2.63 3.17 2.63]

$[X]^t$ = transposed from [X] and it means the vector of the coordinates of **X** in the canonical base of R (a 1×n matrix) [X]: vector of coordinates of **X** in the canonical base of R (a $n \times 1$ matrix)

$$\begin{bmatrix}
0 & 0 & 1 & 0 & 0 & 0 & 0 & 0 & 0 & 0 & 0 & 0 & 0\\
0 & 0 & 2 & 0 & 0 & 0 & 0 & 0 & 0 & 0 & 0 & 0 & 0\\
1 & 2 & 0 & 1 & 0 & 0 & 0 & 0 & 0 & 0 & 0 & 0 & 0\\
0 & 0 & 1 & 1 & 1 & 0 & 0 & 0 & 1 & 0 & 0 & 0 & 0\\
0 & 0 & 0 & 1 & 1 & 1 & 0 & 0 & 0 & 1 & 0 & 0 & 0\\
0 & 0 & 0 & 0 & 1 & 1 & 1 & 0 & 0 & 0 & 0 & 0 & 0\\
0 & 0 & 0 & 0 & 0 & 1 & 1 & 1 & 0 & 0 & 0 & 0 & 0\\
0 & 0 & 0 & 0 & 0 & 0 & 1 & 1 & 1 & 0 & 0 & 0 & 0\\
0 & 0 & 0 & 1 & 0 & 0 & 0 & 1 & 1 & 0 & 0 & 0 & 0\\
0 & 0 & 0 & 0 & 1 & 0 & 0 & 0 & 0 & 0 & 1 & 0 & 0\\
0 & 0 & 0 & 0 & 0 & 0 & 0 & 0 & 0 & 1 & 0 & 2 & 1\\
0 & 0 & 0 & 0 & 0 & 0 & 0 & 0 & 0 & 0 & 2 & 0 & 0\\
0 & 0 & 0 & 0 & 0 & 0 & 0 & 0 & 0 & 0 & 1 & 0 & 0
\end{bmatrix}$$

M^1 (G) : Molecular Pseudograph's Atom Adjacency Matrix

Any local quadratic index has a particular meaning, especially for the first values of k, where the information about the structure of the fragment F_R is contained. High values of k are in relation to the environment information of the fragment F_R considered inside the molecular pseudograph (G).

Atom and atom-type quadratic indices are specific cases of local quadratic indices (for F_R = atom or atom-type). In this sense, the kth atom-type quadratic indices are calculated by summing the kth atom quadratic indices of all atoms of the same atom type in the molecule.

In the atom-type quadratic-indices formalism, each atom in the molecule is classified into an atom-type (fragment), such as heteroatoms, H-bonding acceptor heteroatoms (O, N and S), halogens, aliphatic-chain C atoms, aromatic-ring C atoms, and so on. For all data sets, including those with a common molecular scaffold as well as those with diverse structures, the kth atom-type quadratic indices provide much useful information [34].

Methods

TOMOCOMD-CARDD approach

TOMOCOMD is an interactive program for molecular design and bioinformatics research [29]. The program consists of four subprograms, each dealing with drawing structures (drawing mode) and calculating 2D and 3D molecular descriptors (calculation mode). The modules are named

Computed-Aided 'Rational' Drug Design (CARDD), Computed-Aided Modeling in Protein Science (CAMPS), Computed-Aided Nucleic Acid Research (CANAR) and Computed-Aided Bio-Polymers Docking (CABPD). In this paper we outline salient features concerned with only one of these subprograms: CARDD. This subprogram was developed based on a user-friendly philosophy.

The calculation of total and local quadratic indices for any organic molecule (or any drug-like compound) was implemented in the *TOMO-COMD-CARDD* software [29]. The main steps for the application of this method in QSAR/QSPR can be briefly summarized as follows:

1. Draw the molecular pseudographs for each molecule of the data set, using the software drawing mode. This procedure is carried out by a selection of the active atomic symbols belonging to different groups in the periodic table.
2. Use appropriated atom weights in order to differentiate the molecular atoms. In this work, we used as atomic property the Mulliken electronegativity [35] for each kind of atom.
3. Compute the total and local quadratic indices of the molecular pseudograph's atom adjacency matrix. They can be carried out in the software calculation mode, from which one can select the atomic properties and the family descriptor before calculating the molecular indices. This software generates a table in which the rows correspond to the compounds and columns correspond to the total and local quadratic indices or any other family of molecular descriptors implemented in this program.
4. Find a QSPerR/QSAR equation by using statistical techniques, such as multilinear regression analysis (MRA), neural networks (NN), LDA, and so on. That is to say, one can find a quantitative relation between **P** values and the quadratic indices having, for instance, the following appearance

$$\mathbf{P} = a_0\boldsymbol{q}_0(x) + a_1\boldsymbol{q}_1(x) + a_2\boldsymbol{q}_2(x) + \cdots + a_k\boldsymbol{q}_k(x) + \mathrm{c} \quad (11)$$

   where $\boldsymbol{q}_k(x)$ [or $\boldsymbol{q}_{kL}(x)$] is the kth total [or local] quadratic index, and the $\boldsymbol{a}_k$'s are the coefficients obtained by the linear regression analysis.
5. Test the robustness and predictive power of the QSPR/QSAR equation by using internal and external cross-validation techniques.
6. Develop a structural interpretation of the obtained QSPR/QSAR model using quadratic indices as molecular descriptors.

The descriptors used in order to achieve the theoretical models were the following:

(1) $\boldsymbol{q}_{\boldsymbol{k}}(x)$ are the kth ($k = 15$) total quadratic indices calculated using the kth power of the matrices $[\mathbf{M}^{\boldsymbol{k}}(\mathrm{G})]$ of the molecular pseudograph (G) not considering hydrogen atoms, respectively.
(2) ${}^{\mathbf{E}}\boldsymbol{q}_{\boldsymbol{k}\mathbf{L}}(x)$ and ${}^{\mathbf{H}}\boldsymbol{q}_{\boldsymbol{k}\mathbf{k}}(x)$ are the kth ($k = 15$) local (atom-type) quadratic indices calculated using a kth power of the local matrices $[\mathbf{M}_{\boldsymbol{L}}^{\boldsymbol{k}}(\mathrm{G}, \mathrm{F}i)]$ of the molecular pseudograph (G) not considering hydrogen atoms for heteroatoms (S, N, O), and hydrogen-bonding heteroatoms (S, N, O), respectively.

Data set for QSAR study

The quality of the classification models relies for a great percentage on the quality of the selected training data set. The most critical aspect of the construction of this series is to guarantee a great molecular structural variability. Here we consider a data set consisting of a great number of molecular entities, some of them reported as anthelmintics [2, 4, 36, 37] and the rest with a series of other pharmacological uses [36, 37].

The data set of active compounds was selected by considering representatives of most of the different structural patterns and action mechanisms of anthelmintic activity. In this sense, we included compounds with the following modes of action: (1) cholinergic agonists of the imidazothiazole type (levamisole and butamisole), tetrahydropyrimidines (pyrantel, morantel and oxantel), quaternary ammonium salts (bephenium and thenium) and the pyrimidines (methyridine), (2) cholinesterase inhibitors (dichlorvos and haloxon), (3) GABA agonists (piperazine), (4) glutamate-gated chloride receptor potentiators (ivermectin, abamectin and doramectin), (5) increased calcium permeability (praziquantel), (6) inhibition of microtubule formation, β-tubulin binding (benzimidazoles, albendazole and netobimin), (7) oxidative phosphorylase uncouplers, often called proton ionophores (salicylanilides and substituted

phenols), (8) inhibitors of malate metabolism (diamphenethide), (9) inhibition of phosphoglycerate kinase and mutase (clorsulon) and (10) inhibitors of arachidonic acid metabolism (diethylcarbamzine) [2, 4]. Other compounds that have not been found or defined a specific mode of action, but had been reported as anthelmintics were also included, such as nitroimidazoles and hicantone derivatives.

The inactive compounds were selected in a random way in a great database, with different pharmacological uses (antibacterial, antifungal, antihypertensive, anticancer, hypnotic/sedative, antidepressant and so on). The classification of these compounds as 'inactive' (without anthelmintic activity) does not guarantee that some of these compounds present some anthelmintic activity even not detected.

The data set was divided into two subsets; one of these was used as training (learning) set and the other one as test (prediction) set. The selection was carried out at random, and compounds in the test set were never used in the development of the classification models.

Statistical analysis

Statistical analyses were performed using the STATISTICA software package [38]. The LDA is used in order to generate the classifier functions on the basis of the simplicity of the method [28, 32, 39–41]. In order to test the quality of the discriminant function derived we used the Wilks' λ (U-statistic) and the Mahalanobis distance (D^2). The Wilks' λ statistic is helpful to value the total discrimination and can take values between zero (perfect discrimination) and one (no discrimination). In D^2, D indicates the separation of the respective groups.

The tolerance parameter (proportion of variance that is unique to the respective variable) used was the default value for minimum acceptable tolerance, which is 0.01. Forward stepwise was fixed as the strategy for variable selection. The principle of parsimony (Occam's razor) was taken into account as strategy for model selection. In this connection, we select the model with higher statistical significance but having as few parameters (a_k) as possible.

Finally, the statistical robustness and predictive power of the obtained models was assessed using an external prediction (test) set. In this case, the values of 1 and −1 were assigned to the active and inactive compounds, respectively. The classification of cases was performed by means of the posterior classification probabilities. By using the models one compound can then be classified as active, if $\Delta P\% > 0$, being $\Delta P\% = [P(\text{Active}) - P(\text{Inactive})] \times 100$ or as inactive otherwise. P(Active) and P(Inactive) are the probabilities that the equations classify a compound as active and inactive, respectively. The probability that a case belongs to a particular group is basically proportional to the Mahalanobis distance from that group centroid. In closing, the posterior probability is the probability, based on our knowledge of the values of other variables, that the respective case belongs to a particular group.

Biological activity and in vivo *experiment*

We developed an *in vivo* experiment to measure the chemical effectiveness against *Fasciola hepatica;* in this case, an experimental technique reported in the literature was selected for biological material processing and *F. hepatica* egg extraction [42]. Mitterpak et al.'s technique for host (*Lymnaea cubensis*) invasion was carried out [43]. Afterwards we followed the steps reported by Olazábal et al. [44] to obtain the metacercariae. Metacercariae were conserved at low temperature until the *in vivo* experiment [42].

Balb/c mice were selected as the biological model. Healthy Balb/c mice of both sexes and food were purchased from the 'Centro Nacional de Animales de Laboratorio (CENPALAB)', Cuba. Quarantine, labeling, acclimatization and good maintenance conditions of animals were strictly obeyed [42, 45].

The CBQ organic synthesis laboratory synthesized the compounds **G-1**, with 98% purity. This chemical was tested in order to evaluate their effectiveness against *F. hepatica* according to the following experimental design (see also Table 4).

Table 4. Experimental design.

Product	Dose (mg/kg)	Safety index
G-1	5	4
	15	1.47

Safety index = maximum tolerated dose/applied dose.

Three treatment groups with five mice per group were created. One group (infected control group) was treated with Miglyol 810N (administration vehicle). The second group was neither infested nor treated. The remaining group was treated with **G-1**.

The compound (**G-1**) was previously diluted in 10 ml of Miglyol. All mice received 0.2 ml of **G-1**, through an intraperitoneal route. Mouse invasion with metacercariae of *F. hepatica*, 2 weeks old, 14 days before drug administration, was carried out by Corba et al.'s method [46]. The effectiveness was evaluated based on: (1) determination of the $E\%$ index. This is a quantitative indicator of effectiveness introduced by Steward [47] and defined as $E\% = [(X\text{C}–X\text{T})/X\text{C}] \times 100$ [48]. Here $E\%$ is the percentage of effectiveness, XC is the average amount of *Fasciola* in the control group and XT is the average amount of *Fasciola* in the treated group. The effectiveness was measured based on the elimination or not of *F. hepatica*, in its juvenile stage, as shown by laboratory diagnostics, using the helminthological necropsy on day 7 after the inoculated treatment [46]. (2) Determination of the hepatic index [49], by use of the formula $A = (B/C) \times 100$. In this case, A = hepatic index, B = liver weight and C = body weight. (3) Degrees of lesions of the liver [46]. (4) Spleen relative weight [50]. (5) Intensity of invasion making use of the formula $\text{I.I} = A/B$, where A = total amount of parasites, B = total amount of positives. (6) Extension of invasion by use of the formula $\%\text{E.I} = [\text{T}(t)/\text{T}(a)] \times 100$, where %E.I = percent of invasion extensity, T(t) = number of total positives, T(a) = total of infected animals [51]. (7) Gain of weight (final weight) − (initial weight).

From these different effectiveness indexes [49–51], the $E\%$ index was selected. We used this index in spite of the existence of other (more recently defined) effectiveness parameters because it is a direct expression of effectiveness that one can compare with $\Delta P\%$.

Results and discussion

Development of the classification model

The classification model obtained is given below together with the LDA-statistical parameters:

$$\begin{aligned}\textit{Class} = {} & 2.9161 + 0.014607\,{}^{\mathbf{E}}q_0(\mathrm{x}) - 0.13209\,{}^{\mathbf{E}}q_{1\mathrm{L}}(\mathrm{x}) \\ & + 0.035869\,{}^{\mathbf{E}}q_{2\mathrm{L}}(\mathrm{x}) - 1.55761x10^{-4\mathbf{E}}q_{6\mathrm{L}}(\mathrm{x}) \\ & + 8.21019x10^{-9\mathbf{E}}q_{13\mathrm{L}}(\mathrm{x}) + 0.230519\,{}^{\mathbf{H}}q_{1\mathrm{L}}(\mathrm{x}) \\ & - 0.343107\,{}^{\mathbf{H}}q_{3\mathrm{L}}(\mathrm{x}) + 0.05896\,{}^{\mathbf{H}}q_{5\mathrm{L}}(\mathrm{x}) \\ & - 2.65979x10^{-3\mathbf{H}}q_{7\mathrm{L}}(\mathrm{x}) \qquad (12)\end{aligned}$$

$$N = 291 \qquad \lambda = 0.48 \qquad D^2 = 4.30$$
$$F(9.281) = 33.542 \qquad p < 0.0000$$

where N is the number of compounds, λ is the Wilks statistic, D^2 is the squared Mahalanobis distance and F is the Fisher ratio.

The training set involved 148 active (anthelmintic) compounds and 143 inactive ones. In this set, the obtained model (Equation 12) classified correctly 95.95% of active and 84.62% of inactive compounds, for a global good classification of 90.37%. Table 5 depicts the results of the classification for the training set.

False active compounds are those inactive ones that the model classifies as active, and false inactive compounds are active ones classified as inactive by the model. The percentages of false active and false inactive compounds in the training set are 2.06% (6/291) and 7.56% (22/291), respectively.

An important point of view to accept or reject a model like Equation 12 is the statistics for the external prediction set [52]. The discriminant model correctly classifies 89.23% and 87.09% of active and inactive compounds in the test set, in that order, for a global classification of 88.18%. The percentages of false active and false inactive compounds in the test set are 5.51% (7/127) and 6.29% (8/127), respectively. In Table 6, we give the classification of compounds in this set.

Development of the discriminant functions to predict the mode of action of anthelmintic drugs

In order to develop a QSAR model that permits to predict the main modes of action of the anthelmintic drugs selected as active with the use of the discriminant model (Equation 12), we used a series of the five more representative and studied action modes of the anthelmintic compounds. The targets selected to develop this *in silico* study contain three pharmacological targets 'coupled' to ion channels and another two unrelated action places (at least directly) with ion channels. The linear classification functions to

Table 5. Results of the classification of compounds in the training set.

Compounds	$\Delta P\%$[a]	Compounds	$\Delta P\%$[a]	Compounds	$\Delta P\%$[a]
Training active group					
Tetrachloromethane	96.99	Nitroclofene	−35.68	Diamphenetide	84.86
Perchloroethane	97.58	Nitroscanate	40.66	Miracil C	21.13
Antimony sodium thioglycollate	84.64	G-572	85.78	Dimantine	93.12
Tartaric acid	33.54	Resurantel	90.66	Alazanine triclofenate	71.38
Metrifonate	26.18	Dichlorophen	93.92	Closantel	94.40
Chlorobutane	90.45	Phenzidole	87.63	Becanthone	23.29
Disophenol	32.59	Cyclobendazole	68.43	Dithiazanine iodide	65.66
Stibomen	83.56	Oxantel embonate	69.97	Methylrosanilunium chloride	33.06
Lindane	86.80	Eliminoxy	95.65	Bunamide	94.05
Dimethylpiperazine	6.71	Parbendazole	64.28	Pyruinium	70.75
Fospirate	99.96	Amidantel	32.41	Agrimophol	99.62
Oltipraz	93.64	Mirasan	70.79	Desoine	98.41
Metyridine	69.72	SRC-4402	61.74	Tymoloverm	99.08
Certuna	70.12	Nocodazole	34.21	Pretamazium iodide	85.64
Butonate	80.55	Tolibenzate	95.13	Chuanliansu	16.04
Punicine	81.13	Diphenan	77.42	Hedaquinium chloride	93.81
Antienite	34.75	Haloxon	44.78	Dryocrassin	62.70
Carbendazim	43.06	Cambendazole	30.26	Phenithionate	76.38
Wormin	50.66	Ftalofyne	89.55	Abamectin A	39.83
Thiabendazole	43.43	Coralox	68.15	Abamectin B	80.16
Lobendazole	69.16	Thiophanate	68.49	Amocarzine	86.29
Bromothymol	93.43	Evultin	97.30	Antimony potassium tartrate	98.51
p-Cymine	96.13	Brotianide	93.85	Aspidin	93.80
Acidum kainicum	57.74	Afesal	57.34	Aspidinol	83.27
Ascaridole	83.53	Furodazole	50.91	1,4-Bis(trichloromethyl)benzene	97.52
Geraniol	74.17	Fenbendazole	58.47	Bithionol	80.78
Eucalyptol	96.39	Santolactone	95.69	Carvacrol	95.19
R 8231	57.43	Ticarbodine	98.22	Embelim	95.28
Antafenite	61.44	Butamisole	73.81	Epsiprantel	87.92
Thiacetaisamide	−7.87	Spirazine	−32.06	Acid filix (b)	99.11
Tetramisole	57.95	Hydroxypethidine	74.39	Acid filix (c)	99.05
Levamisole	57.95	Lubisan	82.05	Glycarsamide	84.12
Vincofos	90.60	Meclorazepam	34.36	Hectolin	88.16
Niclofolan	−51.81	Flubendazole	81.72	α-Kosin	59.40
Bromofenofos	73.85	RP 12869	33.88	β-Kosin	69.16
Feniodium chloride	91.05	Egressin	90.27	Mibbemycin A3	85.37
Phenotiazine	95.11	Artemether	68.64	Mibbemycin A4	84.90
Nitazoxanide	−28.80	Bephenium hydroxynapthoate	71.43	Moxidectin	63.57
Bendamizole	10.43	Piperamide maleate	22.87	Naphthalene	96.13
Tioxidazole	28.62	Imcarbofos	−15.45	2-Naphthol	93.12
Phoxim	20.42	Etibendazole	42.03	Nicotine	22.71
Albendazole	41.10	Agrimonulide	82.82	Nitroxynil	5.60
Anthiolimine	47.72	Flurantel	97.60	Paraherquanude	57.05
Morantel	57.39	Amphotaline	86.00	Thymol	94.57
Cetovex	57.40	Difesyl	62.43	Rafoxanide	92.40
4-Hexylresorcinol	94.67	Praziquantel	89.37	α-Santonin	95.69
Pexantel	66.78	153 C 51	86.78	Tenium closylate	50.59
Butynorate	95.33	Trichlorophen	95.55	Quinacrine	42.81
Oxyclozanide	86.44	Miracil B	52.42		
Hexachloropheni-monophosphate	32.96	Lucanthone	56.11		

Table 5. (Continued)

Compounds	$\Delta P\%$[a]	Compounds	$\Delta P\%$[a]	Compounds	$\Delta P\%$[a]
Training inactive group					
Amphotericin B	−94.67	Doxorrubicine	−94.86	Aminopyrine	16.67
Melphalan	−27.62	Hydroxyurea	−90.90	Trimethoprin	−85.26
Busulfan	−89.81	Tolbutamide	−66.40	Dipyridamole	−100.00
Streptozocin	−97.53	Acetohexamide	−34.23	Theophyline	−38.71
Clorzotozine	−97.46	Chlorpropamide	−72.78	Papaverine	10.75
Methotrexate	−99.14	IPTD	−87.75	Gentamicine	−99.97
Fluorouracil	−99.45	Carbutamide	−84.35	Ticarcillin	−18.97
Floxundine	−64.46	Metahexamide	−61.22	Furosemide	−86.01
Chlorodeoxyuridine	−68.26	Glibenclamide	−92.46	Sedormid	56.04
Bromodeoxyuridine	−69.16	Ceftriaxone	−99.98	Clozapine	36.92
Trimidine	−59.14	Gliburide	−92.84	Periciazine	−1.76
Indoxuridine	−69.32	Gliburnuride	−54.91	Nitrazepam	20.02
Trifluoromethyl deoxyuridine	−3.07	Vinblastine	−1.17	Brorizolam	−5.28
Citanabine	−92.06	Azatioprine	−99.08	Lormetazepam	23.97
Azaundine	−96.39	Ergotamine	30.06	Hydroxyzine	−31.94
Mercaptopurine	−38.46	Cisplatin	−94.97	Zopicolone	−85.57
Naphtaline	18.92	Procarbazine	−94.28	Piritinol	−82.19
Ampicillin	−46.32	Vindesina	−67.03	Carbucysteine	−32.02
Amoxicillin	−59.09	Adnamicina	−66.31	Ganciclovir	−99.82
Carbenicillin	17.22	Urecyclic mustard	8.68	Ranitidina	−88.71
Meticillin	−51.70	TEM	−87.26	Labetalol	−50.43
Oxacillin	−40.41	Tiotepa	−3.39	Atenolol	−38.57
Dicloxacillin	−48.20	HMN	−94.51	Betaxolol	−12.61
Cloxacillin	−47.70	Pentamethyl melamine	−97.47	Bisaprolol	−40.79
Floxacillin	−48.19	Carmustine	−52.77	Carteolol	36.03
Piperacillin	−58.27	Dacarbazine	−92.61	Carvediol	−84.39
Nitrofurantoin	−65.81	Clindamycin	−63.26	Timolol	−96.11
Cefazolin	−99.54	Tetracycline	−41.24	Nifuratel	−64.35
Cefalexin	−59.76	Acyclovir	−98.87	Ketoconazole	−30.79
Cefradin	−39.59	Alupurinol	−36.65	Capreomycin	−100.00
Cefamandole	−99.31	Thioguanine	−76.39	Pentostatin	−99.63
Cefalotin	12.43	Mitoxantrone	−99.99	Vinorelbine	−1.97
Aurotioglucose	−62.06	Zalcitabine	−50.52	Nifenazone	48.87
Mephenesin	−99.94	Pentaquine	−34.43	Protacine	−6.80
Chloramphenicol	−78.34	Probenecid	−33.82	Carbamazepine	42.73
Isoniazide	−94.64	Melphalan	−27.62	Pirifibrate	44.37
Rifampicine	−92.43	Cimetidine	−94.33	Zidovudine	−99.36
Dapsone	−30.72	Acebutolol	6.04	Piperacetazine	−11.70
Sulfuxona	−99.82	Reserpine	−40.38	Mexiletim	10.30
Tiosemicarbazone	−26.63	Carbimazole	36.41	Procainamide	17.51
Sulfanilamide	−51.74	Primidone	22.16	Nimodipine	43.48
Sulfisuxazol	−64.73	Chlorothiazide	−99.52	Isosorbide dinitrate	−64.78
Sulfamethoxypyridazine	−95.52	Chlortetracycline	−53.00	Nitroglycerin	−88.20
Sulfapyridine	−45.84	Caffeine	−64.79	Tetranitrate	−98.01
Sulfaguanidine	−95.84	Dipyrrone	−81.89	Hidralazine	−97.37
Prontosil	−79.47	Isoprenaline	−0.24	Minoxidil	−67.00
Primaquine	−73.87	Methaminodiazepoxide	−48.60	Pirazinamide	−29.79
Dauronobicine	−65.03	Metapyrilene	2.43		

[a]$\Delta P\% = [P(\text{Active}) - P(\text{Inactive})] \times 100$ (see Methods).

Table 6. Results of the classification of compounds in an external prediction set.

Compounds	$\Delta P\%$[a]	Compounds	$\Delta P\%$[a]	Compounds	$\Delta P\%$[a]
Test active group					
Tetrachloroethylene	92.91	Clioxanide	91.66	Arecoline	61.71
Dichlorvos	78.71	Dribendazole	58.80	Acid filix (a)	99.17
Piperazine	−70.39	Domoic acid	59.73	Gentian violet	49.24
Niridazole	−86.81	Mebendazole	61.18	8-Hydroxyquinoleine	78.07
Bitoscanate	42.88	Benacyl	34.75	Dichlorophenersine	77.15
Methylarecaidine	61.71	Santoperonim	99.40	Mandelic acid isoamyl ester	88.82
Sodium antimony dimethylcysteine tartrate	91.86	Dibutyltin dilarate	99.96	Naftalofos	75.13
Iodothymol	93.42	Pararosaniline embonate	91.64	Trichlorfon	26.18
Diethylcarbamazine	20.73	Bemosat	66.51	Arsamilate	97.95
Pyrantel	55.59	Salantel	91.98	Kainic acid	57.74
Clorsulon	−86.39	Febantel	10.79	Hexachlorophene	88.57
Stibophen	−99.90	Miracil A	55.85	Dibromsalam	91.91
Oxibendazole	38.57	Hycanthone	−40.72	Tetrachloro-difluoroethane	98.94
Carbantel	92.41	Diospyrol	54.60	Diamphenethide deacetylated (metab)	57.06
Crufomate	53.55	Desaspidin	96.12	Ivermectin	78.56
Niclosamide	45.87	Bidimazium iodide	70.46	Doramectin	90.49
Ontianil potassium	93.82	RO 2-9009	91.91	Milbemycin D	94.83
Atractyl	86.37	Teroxalene	85.48	Dymanthine	93.12
Triclabendazole	49.28	Stilbazium iodide	84.15	Tribromsalam	90.54
Styrylpyridinium chloride	87.37	Netobimin	−84.34	Bromoxanide	97.44
Coomafos	56.45	Artesunate	82.70	Tetrachloroethane	90.19
Oxamniquine	−66.02	Alantolactone	96.50		
Test inactive group					
Mefenamic acid	96.48	Pentamidine	−51.43	Bumetanide	−86.48
Deoxyundine	−64.24	Celiprolol	−1.78	Trapidil	−53.16
Azanibine	−69.80	Penicillamine	72.18	Nizatidine	−96.09
Cefapirine	−57.62	Oxprenolol	−21.97	Saccharin	−52.24
Cefoxilin	−77.15	Metronidazole	−83.71	Isradipine	−13.35
Sulfamethoxazole	−78.28	Teniposide	−83.99	Clofibrate	94.28
Sulfacetamide	−49.19	Isosurbide mononitrate	−46.71	Neomycin	−100.00
Phenytoin	82.94	Propatylnitrate	−84.38	Hachimycin	−33.26
Sulfadiazine	−79.99	Guanitidine	−37.93	Glycobiazol	−79.38
Sulfamethazine	−77.91	Sumatriptan	−85.62	Gobad	−85.51
Sulfathazole	−74.24	Taurocholic acid	−76.31	Taurultam	−92.09
Tolazamide	−70.63	Sildenafil	−97.75	Noxytiolin	−92.93
Sucrida	−90.13	Ciprofloxacin	−74.42	Thiram	−40.01
Mitomycin	−90.92	Bosentan	−99.18	Sulcimid	−77.30
Epirubicin	−99.59	Remikiren	−60.78	Solupront	−97.27
Acetazolamide	−93.84	Halazepan	98.61	Septosil	−93.34
Etoposide	−55.32	Lamotrigine	−82.58	Ibuprofen	95.04
Benazepril	72.05	Sultopride	−82.71	Cintramide	−40.39
Meprobamate	−11.07	Acarbose	−100.00	Triapride	−91.18
Novobiocin	−32.90	Gramsetron	−36.08	Flutizenal	−16.01
Loprazolam	−90.31	Bufeina	77.10		

[a]$\Delta P\% = [P(\text{Active}) - P(\text{Inactive})] \times 100$ (see Methods).

Table 7. Squared Mahalanobis distance (D^2) among groups (modes of action) and percentage of good classification (%) for the training set.

	(NAA)	(AchI)	(GR)	(t)	(H)		%	(NAA)	(AchI)	(GR)	(t)	(H)
(NAA)	0	25.33	32.49	4.67	9.59	(NAA)	100	14	0	0	0	0
(AchI)		0	54.73	8.54	26.97	(AchI)	80	0	8	0	2	0
(GR)			0	34.36	26.60	(GR)	100	0	0	8	0	0
(*t*)				0	8.76	(*t*)	95.45	0	1	0	21	0
(H)					0	(H)	94.73	0	0	0	1	18
						Total	94.52	14	9	8	24	18

describe the main mode of action of the anthelmintic drugs are given below together with their statistical parameters

$$\text{Nicotine AcetylChol. Agonist (NAA)} = -5290193 + 0.075125\boldsymbol{q}_0(\text{x}) - 0.1256^{\mathbf{E}}\boldsymbol{q}_{0\text{L}}(\text{x}) + 0.006242^{\mathbf{E}}\boldsymbol{q}_{2\text{L}}(\text{x}) \quad (13)$$

$$\text{AcetylCholinest.Inh.(AchI)} = -17.98172 + 0.02890\boldsymbol{q}_0(\text{x}) - 0.25641^{\mathbf{E}}\boldsymbol{q}_{0\text{L}}(\text{x}) + 0.068557^{\mathbf{E}}\boldsymbol{q}_{2\text{L}}(\text{x}) \quad (14)$$

$$\text{GluCl Receptor (GR)} = -32.7744 + 0.182145\boldsymbol{q}_0(\text{x}) - 0.01036^{\mathbf{E}}\boldsymbol{q}_{0\text{L}}(\text{x}) - 0.018637^{\mathbf{E}}\boldsymbol{q}_{2\text{L}}(\text{x}) \quad (15)$$

$$\beta\text{-Tubulin (t)} = -7.63587 + 0.0512949\boldsymbol{q}_0(\text{x}) - 0.139856^{\mathbf{E}}\boldsymbol{q}_{0\text{L}}(\text{x}) + 0.02869^{\mathbf{E}}\boldsymbol{q}_{2\text{L}}(\text{x}) \quad (16)$$

$$\text{H-Ionophores (H)} = -8.794881 + 0.03853\boldsymbol{q}_0(\text{x}) + 0.193079^{\mathbf{E}}\boldsymbol{q}_{0\text{L}}(\text{x}) - 0.017196^{\mathbf{E}}\boldsymbol{q}_{2\text{L}}(\text{x}) \quad (17)$$

$$N = 73 \qquad \lambda = 0.034$$
$$F(12, 174) = 37.405 \quad p < 0.0000$$

We use a data set of 93 compounds, for which a specific action mode has been reported. It was randomly split in two subsets, one of them (training set) with 73 compounds and the other (test set) with 20 compounds. The obtained model classifies correctly 94.52% (4/73) and 80.00% (4/20) of the compounds in the training and test set, respectively. Table 7 shows the squared Mahalanobis distances (D^2) between the groups and the classification matrix for the training set. In addition, Table 8 depicts the results for both series (training and test sets) when the discriminant function was used.

In silico *search for anthelmintic compounds like a lead generation procedure*

The massive cost involved in the development of new drugs, together with the low effectiveness of traditional assays in drug discovery highlights the need for a 'sea change' in the drug-discovery paradigm. Predictive *in silico* models could be used for the desired-property identification, accelerating the selection process of leads and predicting their modes of action [53]. One of the most important features of any QSAR model is its ability to predict the desired property for new compounds from databases of chemicals [28]. Computational *in silico* screening of large databases considering the use of such models has emerged as an interesting alternative to high-throughput screening (HTS) and an important drug-discovery tool [54, 55]. With the aim of proving the possibilities of the *TOMOCOMD-CARDD* approach to detect new leads, we performed a simulated virtual screening of anthelmintic drug-like compounds, whose structures are given in Figure 1 and Tables 9 and 10 [56–64].

First, we select compounds for which anthelmintic activity has been reported in international patents [56–60]. The first compound (**I**), named dioxapyrrolomycin, has been patented as a wide-spectrum anthelmintic [56]. It was classified as active by Equation 12 and was predicted as oxidative phosphorylase uncouplers (H-ionophores). This could be related with the protonic H atom in the pyrrol ring. The second and the third compounds (**II, III**) have successful anthelmintic

Table 8. Results of the classification of anthelmintic compounds for the training and test series.

Compound[a]	(NAA)[b]	(AChI)[b]	(GR)[b]	(t)[b]	(H)[b]	Compound[a]	(NAA)[b]	(AChI)[b]	(GR)[b]	(t)[b]	(H)[b]
Nicotinic AcetylCholine Agonist (NAA)											
Metyridine	87.60	0.00	0.00	8.89	3.51	Butamisole	53.06	0.06	0.00	46.23	0.65
Levamisole*	82.99	0.00	0.00	16.39	0.62	Bephenium-hydroxynaphthoate	97.37	0.00	0.00	2.23	0.40
R 8231	71.32	0.01	0.00	26.96	1.71	Morantel*	85.80	0.00	0.00	13.67	0.52
Antafenite	78.94	0.01	0.00	20.62	0.44	Bemosat	88.41	0.00	0.00	7.65	3.93
Tetramisole	82.99	0.00	0.00	16.39	0.62	Difesyl tenium	68.36	0.00	0.02	8.87	22.76
Antienite*	55.95	0.04	0.00	43.05	0.96	Closylate stilbazium	94.29	0.00	0.00	5.17	0.54
Pyrantel	83.63	0.00	0.00	15.71	0.66	Iodide	97.72	0.00	0.67	1.61	0.00
Oxantel embonate	92.02	0.00	0.00	4.17	3.81	Arecoline	68.90	0.00	0.00	21.19	9.91
Styrylpyridinium Chloride	94.29	0.00	0.00	5.28	0.43						
AcetylCholinesterase Inhibitors (AChI)											
Trichlorfon*	0.17	0.02	0.00	3.41	96.40	Imcarbofos	0.00	99.84	0.00	0.16	0.00
Fospirate	0.02	80.10	0.00	19.64	0.25	Dichlorvos*	1.39	55.91	0.00	1.78	40.91
Famophos	0.00	99.13	0.00	0.87	0.00	Uredofos	0.00	100.00	0.00	0.00	0.00
Haloxon*	0.00	94.79	0.00	5.18	0.02	Diuredosan	0.00	99.88	0.00	0.12	0.00
Vincofos	4.84	1.11	0.00	74.10	19.94	Crufomate*	15.70	0.50	0.00	78.81	4.99
Coomafos	0.01	91.94	0.00	8.04	0.00	Naftalofos	0.41	44.70	0.00	54.76	0.13
Coralox	0.00	98.30	0.00	1.70	0.00	Butonate*	0.31	69.82	0.00	28.13	1.75
Metrifonate*	0.17	0.02	0.00	3.41	96.40	Zilantel	0.00	98.57	0.00	1.43	0.00
GluCl Receptor (GR)											
Mibbemycin A3	1.81	0.00	96.06	0.73	1.40	Doramectin	0.00	0.00	100.00	0.00	0.00
Mibbemycin A4	3.59	0.00	91.11	1.71	3.59	Milbemycin D	0.91	0.00	98.56	0.12	0.40
Moxidectin	0.02	0.00	99.96	0.01	0.02	Abamectin A	0.00	0.00	100.00	0.00	0.00
Ivermectin	0.00	0.00	100.00	0.00	0.00	Abamectin B	0.00	0.00	100.00	0.00	0.00
β-Tubulin Inhibitors (t)											
Febantel	1.47	4.31	0.01	70.66	23.56	Furodazole	48.92	0.06	0.00	49.58	1.43
Thiabendazole*	45.10	0.06	0.00	54.33	0.52	Oxfendazole	5.05	5.75	0.00	88.85	0.35
Lobendazole	22.73	0.39	0.00	75.27	1.62	Dribendazole	27.71	0.30	0.00	70.72	1.26
Bendamizole	24.09	0.75	0.00	75.02	0.14	Flubendazole	10.64	0.59	0.00	76.56	12.20
Triclabendazole*	21.69	0.01	0.00	28.04	50.25	Benacyl	7.37	2.86	0.00	88.86	0.91
Tioxidazole	16.79	0.47	0.00	78.27	4.48	Etibendazole	7.27	0.19	0.00	46.52	46.01
Oxibendazole	17.39	0.44	0.00	77.75	4.42	Albendazole sulphoxide	4.12	5.56	0.00	89.50	0.82
Mebendazole*	21.22	0.52	0.00	77.03	1.22	Fenbendazole*	25.01	0.41	0.00	73.60	0.98
Cyclobendazole	42.57	0.10	0.00	56.13	1.20	Bisbendazole	8.15	9.31	0.02	82.50	0.01
Parbendazole	36.77	0.14	0.00	61.60	1.49	Luxabendazole	0.00	99.14	0.00	0.86	0.00
Nocodazole	8.25	2.05	0.00	88.23	1.47	Triclabendazole sulphoxide	27.43	0.05	0.00	47.01	25.52
Cambendazole	3.61	11.19	0.00	85.10	0.09	Benomyl	5.80	4.10	0.00	89.46	0.64
Thiophanate	1.88	9.88	0.00	86.06	2.18	Carbendazim	22.91	0.32	0.00	74.21	2.56
Albendazole*	21.00	0.40	0.00	76.22	2.37						
Proton Ionophores (H)											
Salantel	4.04	0.00	0.07	1.00	94.88	Brotianide	21.96	0.02	0.00	31.93	46.09
Niclofolan*	0.05	0.00	0.00	0.78	99.17	Afesal	1.70	1.56	0.00	55.17	41.57
Trichlorophen	5.76	0.00	0.12	0.22	93.89	Ticarbodine	4.99	0.00	0.00	4.64	90.37

Table 8. (Continued)

Compound[a]	(NAA)[b]	(AChI)[b]	(GR)[b]	(t)[b]	(H)[b]	Compound[a]	(NAA)[b]	(AChI)[b]	(GR)[b]	(t)[b]	(H)[b]
Bromofenofos	0.19	0.02	0.00	3.67	96.12	Flurantel	0.00	0.00	0.00	0.00	99.99
Rafoxanide*	33.58	0.00	0.02	17.36	49.04	Bromoxanide*	0.13	0.00	0.01	0.11	99.75
OK sinid	0.03	0.01	0.00	1.19	98.77	Tribromsalam	22.38	0.00	0.00	9.74	67.87
Oxyclozanide	0.05	0.00	0.00	0.08	99.88	Hexachlorophene	0.04	0.00	0.00	0.01	99.95
Niclosamide	2.40	0.02	0.00	11.91	85.67	Closantel	14.99	0.00	0.57	2.27	82.17
Hexa-chlorophenimonopho-sphate*	0.00	0.00	0.00	0.02	99.98	Dibromsalam*	35.12	0.00	0.00	15.00	49.87
Nirtroclofene	0.06	0.00	0.00	0.86	99.08	Desaspidin	7.42	0.00	3.03	1.62	87.92
Resurantel	39.44	0.00	0.00	12.28	48.28	Bithionol	0.63	0.00	0.00	0.22	99.15
Dichlorophen	30.96	0.00	0.00	1.71	67.33						

[a]Compounds marked with * were used in the external test set.
[b]Percentage of probability with which the drug is predicted to be anthelmintic having Nicotinic AcetylCholine Agonist (NAA), AcetylCholinesterase Inhibitors (AChI), GluCl Receptor (GR), β-Tubulin Inhibitors (t) or Proton Ionophores (H), respectively, as mechanism of action using Equations 13–17.

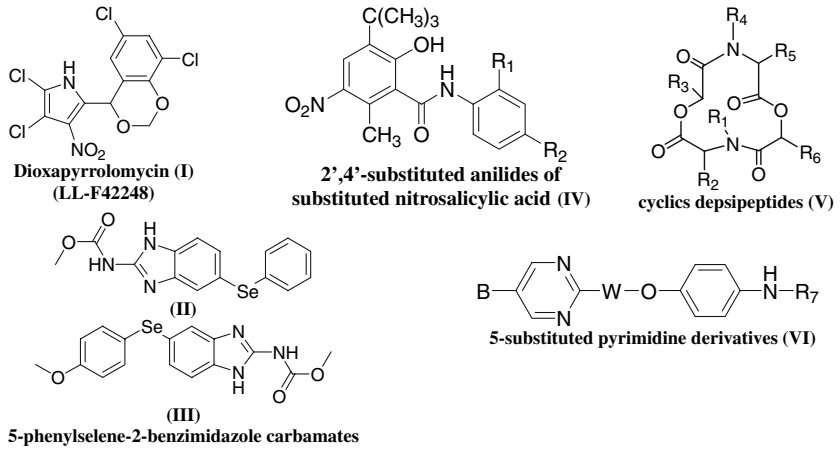

Figure 1. Basic molecular backbone of compounds reported in anthelmintic patent.

and/or fasciolicide activities [57]. They are 5-phenylselene-2-benzimidazole carbamates; they were recognized as inhibitors of microtubule formation by β-tubulin binding. This is a logical result, due to the presence of the benzimidazole ring as the main biophore.

The fourth series of compounds (**IV**-molecular backbone) are 2′,4′-disubstituted anilides of substituted nitrosalicylic acid [58], which have been well predicted as anthelmintic and most of them have also been well classified as oxidative phosphorylase uncouplers. The fifth set (**V**; a new family of cyclic depsipeptides) [59] was correctly selected as anthelmintic by the discriminant function.

Finally, a *subsystem* of 5-substituted pyrimidine derivatives (**VI**) was evaluated. These compounds have been reported as trematocide (mainly fasciolicide) and nematocide [60], and have been predicted as anthelmintic by the obtained model (Equation 12). Most of them were classified as inhibitor of β-tubulin polymerization. However, this result is preliminary and must be corroborated experimentally.

Compounds **I–III**, and the derived series of the molecular backbone **V** and **VI** are completely 'unknown' (the training set used should not contain such compounds) for the developed models; so we can say that their evaluation in the models is

Table 9. Results of the classification of compounds included in anthelmintic patents.

Compound (No and code)[a]		Biological activity			$\Delta P\%$[b]	(NAA)[c]	(AchI)[c]	(GR)[c]	(t)[c]	(H)[c]
I		Wide spectrum			20.83	0.05	0.00	0.00	0.57	99.38
II		Anthelmintic and/or fasciolicide			73.08	47.80	0.08	0.00	51.15	0.97
III					49.36	35.71	0.12	0.00	60.83	3.34
(IV) Substituent		*Haemonchus*	*Fasciola hepatica*	Tolerance						
R_1	R_2			(mg/kg)						
Br	Br	99.8/5	100/5	–	44.06	11.79	0.02	0.01	24.64	63.54
Cl	Cl	100/15	100/5	Sym./100	63.69	27.01	0.00	0.04	13.60	59.35
Cl	Cl	100/5	99/2	Tol./50						
Cl	Cl	14/2	44/1	–						
Cl	Cl-5′	100/15	100/15	Tol./50	48.59	7.54	0.01	0.01	16.43	76.01
Cl	Cl-5′	61/5	0/5	–						
Cl-3′	Cl	100/15	100/15	Tox./50	44.06	7.54	0.01	0.01	16.43	76.01
Cl-3′	Cl	20/5	95/5	Tox./15						
Cl-3′	Cl	–	0/2	–						
Cl-3′	Cl-5′	67,49/15	100/15	Tox./40	47.93	7.54	0.01	0.01	16.43	76.01
Cl-2′	Cl-3′	14/15	–	–	45.78	7.54	0.01	0.01	16.43	76.01
CH_3	Cl	100/15	100/5	Tox./100	61.50	27.93	0.02	0.01	34.92	37.11
CH_3	Cl	99.9/5	0/2	Sym/50						
CH_3	Cl	67/2	–	Tol./25						
CH_3	Br	100/5	100/5	Tox./50	61.15	31.28	0.02	0.01	38.30	30.39
CH_3	Br	38/2	100/5	Sym/50						
CH_3	I	88/5	100/15	Sym/50	60.98	33.69	0.03	0.01	40.49	25.79
CH_3	I	13/2	100/5	–						
CH_3	CI-3′	87/15	0/15	Tox./50	62.10	27.93	0.02	0.01	34.92	37.11
Cl	CH_3	62/15	–	–	51.66	27.93	0.02	0.01	34.92	37.11
Cl-3′	CH_3	80/15	–	–	50.85	27.93	0.02	0.01	34.92	37.11
Cl-3′	CH_3	0/5	–	–						
CF_3	Cl	100/15	100/2	Tox./25	92.40	0.01	0.00	0.00	0.09	99.90
CF_3	Cl	91/5	100/1	Tol./15						
CF_3	Cl	16/2	–	–						
CF_3	Cl	76/1	–	–						
CF_3	Br	100/5	100/5	Tol./35	92.33	0.01	0.00	0.00	0.12	99.86
CF_3	Br	99.8/2	100/2	Tol./20						
CF_3	Br	–	100/1	–						
CF_3	Br	–	97/0.5	–						
Mono-substituted										
Cl-4′		81/15	100/15	–	50.45	23.88	0.02	0.01	35.21	40.88
Cl-4′		65/5	50/5	–						
Cl-4′		0/2	0/2	–						
CF_3-4′		100/15	100/15	–	88.76	0.06	0.00	0.01	0.36	99.58
Br-4′		61/15	100/15	–	49.99	27.05	0.03	0.00	39.06	33.85
Br-4′		–	0/5	–						
I-4′		93/15	0/15	–	49.76	29.37	0.03	0.00	41.63	28.97
I-4′		22/5	–	–						
2′,4′,5′-trichloro		Toxic/15	–	–		39.25	1.57	0.00	0.01	5.06
2′,4′6′-trichloro		73/15	–	–		48.38	1.57	0.00	0.01	5.06

Table 9. (Continued)

(V) Substituents					$\Delta P\%$[b]	(NAA)[c]	(AchI)[c]	(GR)[c]	(t)[c]	(H)[c]
R_1 and R_4			R_2, R_3, R_5 and R_6							
Ethyl			Ethyl		85.81	2.00	13.26	0.00	84.09	0.65
Propyl			Propyl		92.94	26.28	0.57	1.23	71.56	0.36
p-Br-phenyl			CH_2Cl		52.58	0.02	0.04	0.26	1.38	98.30
Phenyl			$(CH_2)_2Cl$		75.11	0.53	0.15	19.21	12.04	68.07
Cyclo-propyl			Ethyl		90.18	2.06	15.49	0.00	82.15	0.30
Cyclo-pentyl			Ethyl		93.37	4.21	8.80	0.04	86.73	0.22
Ethyl			CH_2Cl		27.64	0.02	0.06	0.00	1.95	97.97
(VI) Substituents			Doses (mg/kg)	Post-mortem number of adults fascioles						
B	W	R^7								
Cl	–	H	35	0	42.04	43.13	0.04	0.00	49.64	7.19
Cl	–	CH_3CO–	35	0	63.57	15.87	0.62	0.00	80.77	2.73
Br	–	H	–	–	41.29	44.44	0.05	0.00	50.09	5.42
Cl	–OCH_2CH_2–	CH_3CO–	60	2	42.41	13.37	0.46	0.00	76.18	9.98
Cl	–$(OCH_2CH_2)_2$–	CH_3CO–	75	5	13.91	9.40	0.29	0.00	59.92	30.40
Cl	–$O(CH_2)_3$–	CH_3CO–	35	0	46.72	15.54	0.39	0.00	75.07	9.00
Br	–$O(CH_2)_3$–	CH_3CO–	100	0	46.02	16.18	0.42	0.00	76.55	6.85
CF_3	–$O(CH_2)_3$–	CH_3CO–	50	0	87.99	0.16	0.02	0.00	3.34	96.49
CH_3	–$O(CH_2)_3$–	CH_3CO–	100	0	54.09	25.90	0.30	0.00	71.82	1.98
I	–$O(CH_2)_3$–	CH_3CO–	100	0	45.59	16.66	0.44	0.00	77.34	5.56
Cl	–$O(CH_2)_4$–	CH_3CO–	50	1	50.80	17.97	0.33	0.00	73.62	8.08
Cl	–	=C=S	50	0	8.16	14.23	0.98	0.00	83.64	1.15

[a]The chemical substituents of the compounds represented with numbers or codes are shown in Table 9 and the molecular structure or the backbone are shown in Figure 1.
[b]Anthelmintic activity predicted by Equation 12; $\Delta P\% = [P(\text{Active}) - P(\text{Inactive})] \times 100$.
[c]Percentage of probability with which the drug is predicted to be anthelmintic having NAA, AChI, GR, t, H, respectively as mechanism of action, using Equation 13–17.

equivalent to the discovery of new leads with possibilities in new action mode.

Evidently, the quality of these predictions is not accidental, because the calculations of these descriptors not only give an explanation of the molecule in a global way, but also certain subfragments are considered, which are structural features responsible for the activity. These results confirm that the *TOMOCOMD-CARDD* descriptors used in this work are capable of *a priori* selection/identification and of predicting the mode of action of new lead anthelmintics, starting from a training set consisting of structurally different compounds.

In order to prove even more the possibilities of the *TOMOCOMD-CARDD* approach in the virtual screening of anthelmintic compounds, we have selected a second set of 10 compounds reported in the medical literature as promissory anthelmintics [61–64]. The first compound (**VII**) is a new pro-drug of the benzimidazole type, which has shown activity *in vivo* against *Echinococcus* [61]. This compound was classified as anthelmintic by the obtained model. The compounds **VIII** and **IX** were taken from the medical literature of the last decade [63]. Most of these compounds have been recognized as anthelmintic and classified as cholinergic agonists, which is coherent if we take into consideration the structural features for the cholinergic agonist activity and the modes of action of drugs like pirantel, morantel, and oxantel which have similar structure. The last four compounds (**U-series**) belong to the family of the β-ketoamides [64]. These compounds have shown a

Table 10. Results of the evaluation of compounds reported as anthelmintic.

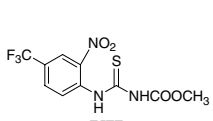

VII

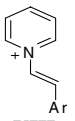

VIII

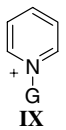

IX

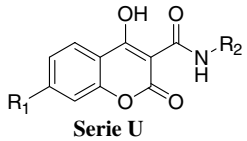

Serie U

No. of code	Structure	MED[a] (mg/kg)	$\Delta P\%$[b]	(NAA)[c]	(AchI)[c]	(GR)[c]	(t)[c]	(H)[c]	
	Ar								
I	–		76.79	0.01	0.01	0.00	0.51	99.48	
II-1	C_6H_5	125	88.61	95.04	0.00	0.00	4.88	0.08	
II-2	o-$CH_3C_6H_4$	15	89.66	95.77	0.00	0.00	4.17	0.06	
II-3	o-ClC_6H_4	31	87.66	92.52	0.00	0.00	7.01	0.47	
III-1	N-allyl	500	81.44	90.46	0.00	0.00	9.22	0.32	
III-2	N-methyl	500	75.46	88.48	0.00	0.00	10.93	0.59	
No of code	Structure		Act. Obs.	$\Delta P\%$[b]	(NAA)[c]	(AchI)[c]	(GR)[c]	(t)[c]	(H)[c]
	R1	R2							
U-86996	H	p-BrC_6H_5		90.72	26.36	0.00	0.00	13.79	59.85
U-87407	Cl	p-BrC_6H_5		89.70	6.60	0.00	0.00	5.10	88.29
			~1 μM						
U-88509	Cl			66.67	0.00	0.00	0.00	0.14	99.86
U-89605	Cl			83.50	0.00	0.00	0.00	0.00	100.00

[a]Anthelmintic activity measured experimentally.
[b]Anthelmintic activity predicted by Equation 12; $\Delta P\% = [P(\text{Active}) - P(\text{Inactive})] \times 100$ (see Methods).
[c]Percentage of probability with which the drug is predicted to be anthelmintic having NAA, AChI, GR, t, H, respectively, as mechanism of action, using Equations 13–17.

potent activity against nematodes (~1 μM against *H. contortus*); they have been predicted as anthelmintic and classified as oxidative phosphorylase uncouplers (H-ionophores). No compound with this kind of structure was included in the training data set and in this sense, its evaluation is equivalent to the discovery of new leads.

At present, data sets of drugs with some pharmacological uses can be assayed in the virtual screening process. This approach is interesting, because compounds selected with this *in silico* procedure have well-established methods of synthesis, although in many cases their toxicological, pharmacodynamical and pharmaceutical behaviors are well known. For this reason, we have selected this method of search for the novel anthelmintic compounds.

We have performed an exhaustive search in the Merck Index [37], Negwer's Handbook [36], and Goodman and Gilman [65] looking for compounds to be evaluated in the models. A reduced group was identified by the discriminant function as a possible anthelmintic. Well-known drugs, with other pharmacological properties, were selected as possibly anthelmintic by the obtained model. These compounds, identified as active, but not having been reported in the literature as anthelmintic, are now in assay in order to prove their anthelmintic activity experimentally.

Interestingly, one of the compounds selected as anthelmintic was colchicine ($\Delta P\% = 70.57$), which unites to the β-tubulin blocking the polymerization and the formation of the microtubules [66]. Although no reports exist of the use of colchicine as anthelmintic, it has been demonstrated experimentally that anthelmintic benzimidazole competed with the binding site for colchicine in β-tubulin [4].

Experimental results: comparison with the theoretical result and discussion for the case of G-1 molecule

Current research in the Chemical Bioactive Center has been focused on the microcidal potential of 2-furylethylenes. In particular, **G-1** [*Z*-1-bromo-1-nitro-2-(5-bromo-fur-2-yl)ethylene] has shown a pronounced double effect (antifungicidal/antibacterial) [67]. It was therefore of major interest for us to develop a general model for predicting the anthelmintic activity for a given molecular structure, with the major emphasis on the case of 2-furylethylenes.

In this sense, good agreement between the experimental anthelmintic (fasciolicide) activity test and the predicted activities for **G-1** was found. As Tables 11 and 12 depict, compound **G-1** was identified as anthelmintic ($\Delta P = 46.76\%$) by the obtained model (Equation 12) and had an effectiveness greater than 80% at 15 mg/kg. Thus, the model shows an overall 100% efficacy in the experimental assessment. Additionally, **G-1** was predicted as oxidative phosphorylase uncouplers ($P = 0.68\%$). This is a logic result, because each anthelmintic molecule with this mode of action (proton ionophore) possesses a detachable proton and is lipophilic. As can be seen in the molecular structure of **G-1** (see Table 11), the H-atom in the α-carbon of the exocyclic double bond and their lipophilic features (Br atoms, nitro group and aromatic ring) can explain the hypothesis of the mode of action, because this lipid-soluble substance (Log $P_{n\text{-oct/(buffer 7.4)}} = 2.49$ [68]) is capable of carrying protons across a membrane, therefore, may act to uncouple oxidative phosphorylation preventing the production of the proton gradient across the inner mitochondrial membrane. Table 11 shows the position of the proton that is able to dissociate from compound **G-1**. However, these theoretical results must be considered only as preliminary screening results and an experimental corroboration is necessary in the future.

Table 11. Results in the treatment on *Fasciola hepatica* 2 weeks old with **G-1** in Balb/c mice. The location of the dissociating proton (H) is shown in the shaded box.

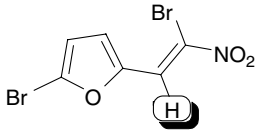

P	Dose (mg/kg)	Number *Fasciola* Mean (±SD)	IE (%)	Weight gain (g) Mean (±SD)	M (%)	Affected liver (%)	Hepatic index Mean (±SD)	Splein relative weight (g) Mean (±SD)	Effectivity E (%)
G-1	5	1 (0.45)	67	0.11 (0.01)	0	71	6.9 (0.2)	1.23 (0.02)	0
	15	0.2 (0.82)	20	1 (0.1)	29	60	7.5 (0.21)	1.16 (0.024)	80
Infected		0.5 (1.7)	50	−1.25 (0.18)	14	50	7.24 (0.05)	1.05 (0.02)	–
		1 (0.54)	33	0.78 (0.08)	63	33	5.8 (0.1)	0.99 (0.03)	–
Control				1.48 (0.07)	–	–	5.8 (0.17)	0.46 (0.02)	–
no infected				0.89 (0.1)	–	–	4.5 (0.17)	0.37 (0.02)	–

P = Product, (±SD) = ±Standard deviation, M = Mortality mice, IE = Invasion extensity.

Table 12. Comparison between experimental (effectivity) and theoretical activity.

Compound	Dose (mg/kg)	E(%)[a]	$\Delta P\%$[b]	(NAA)[c]	(AchI)[c]	(GR)[c]	(t)[c]	(H)[c]
G-1	15	80	46.76	0.06	0.00	0.00	0.26	0.68

[a]Anthelmintic activity measured experimentally (see Methods).
[b]Anthelmintic activity predicted by Equation 12; $\Delta P\% = [P(\text{Active}) - P(\text{Inactive})] \times 100$ (see Methods).
[c]Percentage of probability with which the drug is predicted to be anthelmintic having NAA, AChI, GR, t, H, respectively as mechanism of action using Equation 13–17.

Concluding remarks

Computational – *in silico* – screening has become nowadays an important tool in the development of drug discovery, although it is clear that *in silico* predictive modeling does not represent a panacea for the industry [53]. In this paper, a novel *TOMOCOMD-CARDD* descriptor was used to obtain a quantitative LDA model that discriminates anthelmintic compounds from inactive ones; and to perform another model to classify the anthelmintic compounds taking into consideration their modes of action. The obtained models were significant from the statistical point of view. Virtual screening of drugs was carried out by us to prove the usefulness of the present approach to discover new anthelmintic compounds from 2D chemical-structure databases or combinatorial libraries. Finally, we made an experimental corroboration, using one compound developed in the Chemistry Bioactive Center, of the predictions of our models.

Acknowledgements

The authors acknowledge the anonymous referees for their valuable comments in order to increase the quality of the manuscript. F.T. is grateful for financial support from the Spanish MCT (Plan Nacional I+D+I, Project No. BQU2001-2935-C02-01) and Generalitat Valenciana (DGEUI INF01-051 and INFRA03-047, and OCYT GRUPOS03-173).

References

1. Kohler, P., Int. J. Parasitol., 31 (2001) 336.
2. Martin, R.J., Robertson, A.P. and Bjorn, H., Parasitology, 114 (1997) S111.
3. Pichard, R.K., Vet. Parasitol., 54 (1994) 259.
4. Martin, R.J., Vet. J., 154 (1997) 11.
5. González Díaz, H., Olazábal, E., Castañedo, N., Hernández, I., Morales, A., Serrano, H.S., González, J. and Ramos, R., J. Mol. Mod., 8 (2002) 237.
6. Cioli, D., Parasitol. Today, 14 (1998) 418.
7. Conceicao, M.J., Argento, C.A. and Correa, A., Memorias instituto Oswaldo Cruz, 95 (2000) 375.
8. Liang, Y.S., Coles, G.C. and Doenhoff, M., J. Trop. Med. Int. Health, 5 (2000) 72.
9. Reynoldson, J.A., Behnke, J.M., Pallant, L.J., Macnish, M.G., Gilbert, F., Giles, S., Spargo, R.J. and Thompson, R.C., Acta Trop., 68 (1997) 301.
10. Sangster, N.C. and Gill, J., Parasitol. Today, 15 (1999) 141.
11. Coles, C.C., J. Med. Microbiol., 48 (1999) 323.
12. Moll, L., Gaasenbeek, C.P., Vellena, P. and Borgsteede, F.H., Vet. Parasitol., 91 (2000) 153.
13. Rothwell, J. and Sangster, N., Int. J. Parasitol., 27 (1997) 313.
14. Evans, A.M. and Martin, R.J., Br. J. Pharmacol., 118 (1996) 1127.
15. Martin, R.J., Pharmacol. Therapeut, 58 (1993) 13.
16. Robertson, S.J. and Martin, R.J., Br. J. Pharmacol., 108 (1993)170.
17. Martin, R.J., Br. J. Pharmacol., 84 (1985) 445.
18. Martin, R.J., Parasitology, 147 (1996).
19. Cully, D.F., Wilkinson, H., Vassilitis, D.K., Etter, A. and Arena, J.P., Parasitology, 113 (1996) 191.
20. Redman, C.A., Robertson, A.P., Fallon, P.G., Modha, J., Kusel, J.R., Doenhoff, M.J. and Martin, R.J., Parasitol. Today, 12 (1996) 14.
21. Roos, M.H., Kwa, M.S.G. and Grant, W.M., Parasitol. Today, 11 (1995) 148.
22. McKellar, Q.A. and Kinabo, L.D.B., Br. Vet. J., 147 (1991) 306.
23. Edwards, S.R., Campbell, A.J., Sheers, M., Moore, R.J. and Montague, P.E., Mol. Biochem. Parasitol., 2 (1981) 339.
24. Edwards, S.R., Campbell, A.J., Sheers, M., Moore, R.J. and Montague, P.E., Mol. Biochem. Parasitol., 2 (1981) 323.
25. Schulman, M.D., Ostlind, D.A. and Valentino, D., Mol. Biochem. Parasitol., 5 (1982) 133.
26. Maizels, R.M. and Denham, D.A., Parasitology, 105 (1992) 49.
27. Estrada, E., Environ. Res., 11 (2000) 55.
28. Estrada, E. and Peña, A., Bioorg. Med. Chem., 8 (2000) 2755.
29. Marrero-Ponce, Y. and Romero, V., *TOMOCOMD* software, version 1.0, 2002, Central University of Las Villas. *TOMOCOMD* (*TO*pological *MO*lecular *COM*puter *D*esign) for Windows, version 1.0 is a preliminary experimental version; in the future a professional version can be obtained upon request from Y. Marrero: yovanimp @qf.uclv.edu.cu or ymarrero77@yahoo.es.
30. Marrero-Ponce, Y., Molecules, 8 (2003) 687.
31. Marrero-Ponce, Y., Cabrera, M.A., Romero, V., Ofori, E. and Montero, L.A., Int. J. Mol. Sci., 4 (2003) 512.
32. Marrero-Ponce, Y., Cabrera, M.A., Romero, V., González, D.H. and Torrens, F., J. Pharm. Pharm. Sci., 7 (2004) 186.
33. Marrero-Ponce, Y., Nodarse, D., González-Díaz, H., Ramos, R., Romero-Zaldivar, V., Torrens, F. and Castro, E. Nucleic Acid Quadratic Indices of the "Macromolecular Graph's Nucleotides Adjacency Matrix". Modeling of Footprints after the Interaction of Paromomycin with the HIV-1 ψ-RNA Packaging Region. *CPS: physchem/0401004*.
34. Hall, L.H. and Kier, L.B., J. Chem. Inf. Comput. Sci., 35 (1995) 1039.
35. Cotton, F.A., Adv. Inorg. Chem. Revolucionaria Havana, 1966.
36. Negwer, M., Organic-chemical Drugs and their synonyms. Akademie-Verlag, Berlin, 1987.
37. The Merck Index, Twelfth Edition. Chapman & Hall, New York, 1996.
38. STATISTICA ver. 5.5, Statsoft, Inc., 1999.
39. González-Díaz, H., Marrero-Ponce, Y., Hernández, I., Bastida, I., Tenorio, E., Nasco, O., Uriarte, E.,

Castañedo, N., Cabrera, M.A., Aguila, E., Marrero, O., Morales, A. and Pérez, M., Chem. Res. Toxicol., 16 (2003) 1318.
40. Estrada, E., Peña, A. and Garcia-Domenech, R., J. Comput.-Aided Mol. Des., 12 (1998) 583.
41. Julian-Ortiz, J.V., Gálvez, J., Muños-Collado, C., García-Domenech, R. and Gimeno-Cardona, C., J. Med. Chem., 42 (1999) 3308.
42. Milligen, F.J., Cornelissen, J.B., Guasenbeek, C.P. and Bokhout, B.A., J. Immunol. Met., 213 (1998) 183.
43. Mitterpak, J., Mendéz, M. and Mauri, M., Serie biológica, 30 (1972) 1.
44. Olazábal, E., Morales, A., Serrano, H. and Brito, E., Vet. Méx., 30 (1999) 109.
45. Ping, C. and Hayes, A., Acute toxicity and eyes irritancy: Principles and Methods of Toxicology, Third Edition. Raven Press Ltd, New York, 1994.
46. Corba, J., Velebny, S. and Spaldonova, R., Helminthology, 18 (1981) 43.
47. Steward, J.S., Parasitology, 45 (1955) 231.
48. Wood, I.B., Amaral, N.K., Bairden, K., Duncan, J., Kassai, T., Malone, J.B., Pankavich, J.A., Reinecke, R.K., Slocombe, O., Taylor, S.M. and Vercruysse, J., Vet. Parasitol., 58 (1995) 181.
49. Tsocheva, N., Krustev, L. and Polyakova, O., Helminthology, 27 (1992) 261.
50. Poitou, I., Baeza, E. and Boulard, C., Vet Parasitol., 45 (1992) 59.
51. Espaine, L., Lines, R. and Demedio, J., Manual de Parasitología y enfermedades Parasitarias I. Editorial MES, Habana (1996) 103.
52. Golbraikh, A. and Tropsha, A., J. Mol. Graphic Model., 20 (2002) 269.
53. Watson, C., Biosilico, 3 (2003) 83.
54. Lajiness, M.S., In Rouvray, D.H. (Ed.), Computational Chemical Graph Theory, Nova Science, New York, 1990, pp. 299.
55. Walters, W.P., Stahl, M.T. and Murcko, M.A., Drug Discov. Today, 3 (1998) 160.
56. Conder, G., Kuo, M., Marshall, V. and Zielinski, R., United States Patent 5,643,940 (1997).
57. Flynn, A., United States Patent 4,303,666 (1981).
58. Meek, W., United States Patent 3,949,075 (1976).
59. Scherkenbeck, J., European Patent 0 664 297, A1 (1988).
60. Serban, A., Watson, K., Wilshire, C. and Forsyth, B., United States Patent 4,460,588 (1984).
61. Walchshofer, N., Delabre-Defayolle, I., Paris, J. and Petavy, A.F., J. Pharm. Sci., 7 (1990) 79.
62. Ames, R.A., J. Pharm. Sci., 3 (1991) 293.
63. Ames, J.R., Castognoli, N., Ryan, M.D. and Kavacic, P., Free Rad. Res. Commun., 2 (1986) 107.
64. Ho, N.F.H., Sims, S.M., Vidmar, T.J., Day, J.S., Barsuhn, C.L., Thomas, E.M., Geary, T.G. and Thompson, D., J. Pharm. Sci., 83 (1994) 1052.
65. Goodman, A.G., Goodman, L.S. and Gilman, A., Las bases Farmacológicas de la Terapeutica, 9na Ed. Vol II, McGraw-Hill, New York, 1996.
66. Alberts, B., Bray, D., Lewis, J., Raff, M., Roberts, K. and Watson, J.D., Molecular Biology of the Cell. Third edition. Garland Publishing, Inc., New York and London, 1994.
67. Blondeau, J.M., Castañedo, N., Gonzalez, O., Medina, R. and Silveira, E. Antimicrob. Agents Chemother., 11 (1999) 1663.
68. Cabrera, M.A., González, H., Jiménez, E., Pérez, D.O., Gómez, E. and Castañedo, N., Eur. Bull. Drug Res., 9 (2001) 1.